

70-year anthropogenic uranium imprints of nuclear activities in Baltic Sea sediments

Mu Lin

Department of Environmental Engineering, Technical University of Denmark, DTU Risø Campus, DK-4000 Roskilde, Denmark

Jixin Qiao (✉ jqiqi@env.dtu.dk)

Department of Environmental Engineering, Technical University of Denmark, DTU Risø Campus, DK-4000 Roskilde, Denmark <https://orcid.org/0000-0001-5409-4274>

Xiaolin Hou

Department of Environmental Engineering, Technical University of Denmark, DTU Risø Campus, DK-4000 Roskilde, Denmark

Olaf Dellwig

Department of Marine Geology, Leibniz Institute for Baltic Sea Research Warnemünde, IOW, 18119 Rostock, Germany

Peter Steier

VERA Laboratory, Faculty of Physics, Isotope Physics, University of Vienna, Währinger Straße 17, A-1090 Vienna, Austria

Karin Hain

VERA Laboratory, Faculty of Physics, Isotope Physics, University of Vienna, Währinger Straße 17, A-1090 Vienna, Austria

Robin Golser

VERA Laboratory, Faculty of Physics, Isotope Physics, University of Vienna, Währinger Straße 17, A-1090 Vienna, Austria

Liuchao Zhu

Department of Environmental Engineering, Technical University of Denmark, DTU Risø Campus, DK-4000 Roskilde, Denmark

Research Article

Keywords: U-236, U-233, Baltic Sea, sediment, global fallout, Chernobyl accident, nuclear reprocessing plant, Anthropocene

Posted Date: April 1st, 2021

DOI: <https://doi.org/10.21203/rs.3.rs-383698/v1>

License:  This work is licensed under a Creative Commons Attribution 4.0 International License.

[Read Full License](#)

Abstract

Strongly stratified water structure and densely populated catchment make the Baltic Sea one of the most polluted seas. Understanding its circulation pattern and time scale is essential to predict the dynamics of hypoxia, eutrophication, and pollutants. Anthropogenic ^{236}U and ^{233}U have been demonstrated as excellent transient tracers in oceanic studies, but unclear input history and inadequate long-term monitoring records limit their application in the Baltic Sea. From two dated Baltic sediment cores, we obtained high-resolution records of anthropogenic uranium imprints originated from three major human nuclear activities throughout the Atomic Era. Using the novel $^{233}\text{U}/^{236}\text{U}$ signature, we distinguished and quantified ^{236}U inputs from global fallout (43.3%-50.5%), Chernobyl accident (< 0.9%), and discharges of civil nuclear industry (48.6%-56.7%) to the Baltic Sea. We estimated the total release of ^{233}U (7-15kg) from the atmospheric nuclear weapons testing, and pinpointed ^{233}U peak signal in the mid-to-late 1950s as a potential time marker for the onset of the Anthropocene Epoch. This work also provides fundamental ^{236}U data for Chernobyl accident and early discharges from civil nuclear facilities, prompting worldwide ^{233}U - ^{236}U tracer studies. We anticipate our data to be a broader application in model-observation interdisciplinary research on water circulation and pollutant dynamics in the Baltic Sea.

Synopsis

This work supplements fundamental ^{236}U and ^{233}U source-term data for major human nuclear activities, facilitating regional and worldwide ^{233}U - ^{236}U environmental tracer applications.

Introduction

As the second-largest brackish water body worldwide, the Baltic Sea is a shallow enclosed marginal sea and characterized by a permanent halocline restricting the ventilation of bottom waters.^{1,2} The renewal of deep waters mainly relies on the O_2 -rich saline inflows from the North Sea.^{1,3} Long residence time of saline water (~30 years),⁴ dramatic drop in the frequency of Baltic inflows since the 1980s, and the persistent eutrophication trigger the world's largest hypoxic area and make the Baltic Sea extremely sensitive to anthropogenic pollutants from its highly populated catchment.⁵⁻⁷ Hence, investigation of the transit time and transport pathways of the saline waters in different sub-basins of the Baltic Sea is essential to predict the dynamics of hypoxia, eutrophication, and pollutants.

Our previous studies⁸⁻¹¹ indicate that the Baltic Sea receives radioactive discharges (e.g., ^{99}Tc , ^{137}Cs , ^{129}I , and ^{236}U) from two European nuclear reprocessing plants at Sellafield and La Hague via Baltic inflows. Among these radionuclides, ^{236}U ($t_{1/2} = 23.4$ Myr) is a powerful oceanic tracer owing to its long half-life, high solubility, and long residence time in the ocean.^{12,14,15} Throughout the Atomic Era, significant amounts of ^{236}U have been released to the environment by human nuclear activities, such as global fallout of atmospheric nuclear weapons testing (900 - 2100 kg)^{12,16-18} and deliberate discharges

from Sellafield and La Hague (more than 263 kg)¹⁹. Coupled with ¹²⁹I, the point-like releases of reprocessing-derived ²³⁶U have been utilized to quantify timescales of regional ocean circulation, e.g. the Atlantic waters in the Arctic Ocean.^{20–23}

Reprocessing-derived ²³⁶U is a promising proxy to investigate the Baltic inflows, but it suffers from methodological difficulties in distinguishing it from ubiquitous global-fallout-derived ²³⁶U. Recently, a ²³³U-²³⁶U paired tracer system was proposed to identify emission sources of ²³⁶U.^{8,14,24} This is based on the fact that ²³³U ($t_{1/2} = 0.16$ Myr), another long-lived U isotope, was mostly released from nuclear weapons testing, while almost no ²³³U is produced in commercial nuclear power reactors or reprocessing plants.¹⁴ The representative ²³³U/²³⁶U atomic ratio of global-fallout signal was suggested to be $(1.40 \pm 0.15) \times 10^{-2}$.¹⁴ Discharge data of La Hague and reactor-modeling results indicate that $10^{-8} - 10^{-6}$ is the representative level of ²³³U/²³⁶U atomic ratio for the reactor-related releases.^{14,25,26} Thereby, ²³³U/²³⁶U can be used as a robust fingerprint to quantify the global-fallout-derived and reactor-derived ²³⁶U. However, there is still a knowledge gap in the release history and global inventory of ²³³U, which is critical for its tracer application.

Moreover, the ²³⁶U budget is still an open question in the Baltic Sea due to the unclear input function and limited observation data. Many studies have reconstructed the temporal distribution of ²³⁶U in marine waters from biogenic materials (like corals and shells) and further estimated the ²³⁶U inputs of global fallout and nuclear reprocessing plants into the ocean (**Table S1**).^{14,18,19,27,28} Unfortunately, such efforts do not apply to the Baltic Sea because of the absence of corals and the lack of routine sampling of shells. Hence, anoxic sediments from the deep basins of the Baltic Sea become an alternative promise considering the advantages of single sampling, flexible time scale, and high sample accessibility.

In this work, we resolved 70-year temporal evolution of ²³⁶U and ²³³U in the Baltic Sea from two dated sediment cores collected in the Gotland Basin, the largest Baltic sub-basin, and Landsort Deep, the deepest Baltic sub-basins, respectively (**Figure 1**). The historical ²³⁶U inputs from various sources were quantified with an endmember mixing model. The ²³⁶U budget in the Baltic Sea and the global release of ²³³U from atmospheric nuclear weapons testing were further estimated based on the new ²³⁶U-²³³U dataset.

Materials And Methods

A sediment core 7-MUC4 (L = 30 cm, $\Phi = 10$ cm) was collected at site GB7-4 (57°16.98'N, 20°07.23'E, 241 m water depth) in the central Gotland Basin during a cruise with RV Elisabeth Mann Borgese in December 2018 (EMB201). The core covers a period from the 1940s until 2018. The composite core 11-10MUC2/36-MUC3 is compiled from two sediment cores collected at the same site LD1 (58°38.36'N, 18°16.04'E, 437 m water depth) in the Landsort Deep. Core 11-10MUC2 (L = 49 cm, $\Phi = 10$ cm), collected during the EMB201 cruise, covers the period from ~1957 until sampling in 2018. To extend this sediment record to

~1948, six additional samples from core 36-MUC3 (L = 37.5 cm, Φ = 10 cm), previously obtained during a cruise with the RV Meteor at site LD1 in November 2011 (M86/1a), were added resulting in a composite profile. All sediment cores were collected by a multicorer device, sliced in 0.5-cm or 1-cm resolution on-board, and then freeze-dried and homogenized by an agate ball mill for geochemical and radiochemical analyses.

To investigate the behaviors of natural U in the Gotland Basin and Landsort Deep, water column samples collected by Pump-CTD and sediment porewater samples extracted by rhizons were analyzed for U concentrations.^{29,30} For dissolved U, water column samples after filtration with 0.45 μm syringe filters (SFCA) and porewater samples were immediately acidified to 2 vol% of HNO_3 . For particulate U, 2 L of the water sample was filtered through 0.4 μm polycarbonate filters (Millipore) and the residue was rinsed with 50 mL of ultrapure water to remove remaining salt. To determine total sulfide, porewater and filtrated seawater samples were added to 2 mL reaction tubes containing 20 μL of 20 vol% Zn acetate.

Further details of the analytical methods adopted in this work are provided in the Supporting Information. After total digestion with an acid mixture (HNO_3 : HClO_4 : HF = 1 : 2 : 2, v/v), the sedimentary Al, Mn, U, and stable Pb isotope ratios in Baltic Sea sediment cores were determined by inductively coupled plasma mass spectrometry (ICP-MS, iCAP Q, Thermo Fisher Scientific) or inductively coupled plasma optical emission spectrometry (ICP-OES, iCAP 7400 Duo, Thermo Fisher Scientific). The Hg contents were measured by a direct mercury analyzer (DMA-80; Milestone). The total organic carbon (TOC) contents were determined by the differences between total carbon and total inorganic carbon contents. All element and TOC contents are salt-corrected because of salt contents of up to 30 wt% in some freeze-dried samples.

Besides sedimentary U contents, the concentrations of dissolved and particulate U, O_2 , and sulfide in the water column, as well as the concentrations of dissolved U and sulfide in the porewaters of the sediments, were analyzed. O_2 concentrations in the water column were directly determined using an SBE 911+ CTD (Sea-Bird) equipped with an SBE 43 oxygen sensor. Total sulfide in porewater and water column samples was determined by the Cline method.³¹ The concentrations of dissolved U in water column and porewater samples were measured by ICP-MS coupled to a seaFAST-pico system (Elemental Scientific) as previously applied for Mo and W.³⁰ Except for decomposing of polycarbonate filter by HClO_4 before adding HF during total acid digestion, the U concentrations of the suspended particulate matter from the water column at site LD 1 were analyzed in the same way as the sediment samples.

An optimized radiochemical procedure modified from our previous work was utilized for the determination of $^{236}\text{U}/^{238}\text{U}$, $^{233}\text{U}/^{238}\text{U}$, and $^{233}\text{U}/^{236}\text{U}$ atomic ratios in sediments by accelerator mass spectrometry (AMS), including acid digestion, co-precipitation, and extraction chromatography.^{32,33} As strong acids are able to leach ^{236}U from soil and sediments quantitatively,^{16,34} acid digestion with *Aqua regia* ($\text{HCl}:\text{HNO}_3=3:1$, v/v) rather than total dissolution was adopted in our procedure to deal with gram amounts of sediment samples. About 93% and 84% of ^{238}U in the Gotland Basin and Landsort Deep

cores (obtained by total dissolution using $\text{HNO}_3\text{-HClO}_4\text{-HF}$) were leached by *Aqua regia* digestion, respectively. A leaching experiment on core 7-MUC4 indicates that a single *Aqua regia* digestion is enough to extract >99% of leachable ^{238}U and ^{236}U from the sediments (**Table S2**). To avoid the introduction of extra ^{236}U and ^{233}U from yield tracer, ^{238}U in the *Aqua regia* leachate was used as an intrinsic chemical yield tracer, and our radiochemical procedure provided satisfactory chemical yields (80 - 100%) for ^{236}U and ^{233}U . Nine procedure blanks were prepared following the same analytical protocol along with the sediment samples. Special measures presented in the Supporting Information were implemented for the background control of ^{236}U and ^{233}U .³³ The procedure blanks contained less than 5.3 ng of ^{238}U , 1.8×10^6 atoms of ^{236}U , and 9.6×10^4 atoms of ^{233}U , which is negligible compared with minimum amounts of ^{238}U , ^{236}U , and ^{233}U in the sediment samples except for the lowermost layer. To locate the layer recording the Chernobyl accident signal, ^{137}Cs and ^{241}Am activities in the sediment were directly measured by gamma spectrometry.

The gamma measurements of ^{137}Cs and ^{241}Am and the radiochemical separation procedure for ^{236}U and ^{233}U were performed at the Department of Environmental Engineering in the Technical University of Denmark (DTU-ENV); the AMS measurements of ^{236}U and ^{233}U were carried out at the Vienna Environmental Research Accelerator (VERA) facility in the University of Vienna; and all the other analyses were completed at Leibniz Institute for Baltic Sea Research Warnemünde (IOW).

Results And Discussions

Dating of the Sediment Cores.

As previous studies in the Gotland Basin and Landsort Deep revealed severe limitations in ^{210}Pb dating of sediment cores subjected by pronounced redox dynamics,³⁵⁻³⁷ the age models for the obtained sediment cores in this work were developed by an event-stratigraphic approach (see Details for the Analytical Methods in Supporting Information and **Figure S1-S7**). Specific time markers were identified along the cores through geochemical and radiological analyses, including: Mn enrichments following the Major Baltic Inflows (1978, 1994, 2003, and 2014), Chernobyl-accident-derived ^{137}Cs and ^{241}Am peaks (1986), initial and maximum global-fallout-derived ^{241}Am (1954 and 1963), maximum Pb pollution identified by stable $^{206/207}\text{Pb}$ ratios (1970 - 1978), and onset of modern Hg pollution reflected by Hg/Al ratios (1950). Between these time markers, sedimentation rates vary between 0.25 - 1.44 cm/yr, providing nearly annual or biennial sample resolutions with conventional core slicing. The obtained age-depth relations enable to reconstruct the sedimentary chronology since the 1940s. All geochemical and radiochemical analysis data involved in this work can be found in **Table S3-S6**.

Record of Uranium Contents in the Sediment Cores.

The sedimentary U levels from the Gotland Basin and Landsort Deep (ave. 31.7 and 16.7 mg/kg, respectively) are much higher than other type-localities of sulfidic basins such as the Black Sea and

Cariaco Basin,^{15,38,39} suggesting that the Gotland Basin and Landsort Deep act as effective U sinks during the past ~70 years. Distinct U enrichments appear in both cores especially in the organic-rich sapropel intervals deposited during sulfidic water-column periods (**Figure 2** and **Figure S8**), because soluble U(VI) can be reduced to insoluble U(IV) in reductive condition (e.g., if H₂S is present)⁴⁰ and the formed U(IV) is easily adsorbed on suspended particles and deposited on the seabed. Water-column and porewater profiles obtained in the Gotland Basin and Landsort Deep in 2018 clearly document two scavenging processes of U (see Supplementary Discussions in Supporting Information): i) the redox-driven removal of dissolved U from the sulfidic water column to the sediment as particulate forms;⁴¹ and ii) the diagenesis-driven removal of dissolved U in the sulfidic porewater environment mediated through reductants, facilitating the diffusion of dissolved U from bottom water to the porewater.⁴²⁻⁴⁴ On the other hand, a less effective U burial is observed in the Mn carbonate-rich sections of both cores, which were formed during the hypoxic (O₂ < 2 mL/L ≈ 90 μM)^{2,7,45} water-column periods.³⁶ This difference is most likely related to the limited redox-driven scavenging in the non-sulfidic waters. However, the diagenesis-driven removal should be maintained below the sediment-water interface by the pronounced reducing or even sulfidic conditions, as Al-normalized U concentrations ((0.70 - 19.6) × 10⁻⁴) still strongly exceed the lithogenic background as represented by the upper continental crust (0.33 × 10⁻⁴)⁴⁶.

The aforementioned results indicate that most of natural sedimentary U originates from the dissolved U in the water column. In principle, this should also be valid for soluble ²³³U and ²³⁶U, such as the dissolved fraction of global-fallout-derived ²³³U and ²³⁶U and liquid discharges of reprocessing-derived ²³⁶U. Hence, the anoxic sediments could record the historical compositions of U isotopes in the water column, mostly deep waters where U is efficiently scavenged. It is noteworthy that the sediments may also directly receive atmospheric depositions of particulate ²³³U and ²³⁶U, such as the global fallout from nuclear weapons testing and the regional fallout from the Chernobyl accident. Permanently hypoxic and periodically sulfidic water-column conditions prevent bioturbation and facilitate the preservation of U in its immobilized tetravalent state,⁴² making these ²³³U and ²³⁶U inputs ideal time markers for dating purpose.

Deposition History and Total Release of ²³³U from Global Fallout.

Most measured ²³³U/²³⁸U and ²³⁶U/²³⁸U atomic ratios in both sediment cores are much higher than their natural background (10⁻¹⁴ - 10⁻¹¹ and 10⁻¹⁴ - 10⁻¹⁰, respectively),^{14,47} suggesting anthropogenic ²³³U and ²³⁶U have dominated the Baltic Sea since the mid-1940s. Both cores exhibit very similar temporal distribution patterns for ²³³U/²³⁸U atomic ratios, consisting of a notable peak in the mid-to-late 1950s and a following gradual decrease until 2018 (**Figure 3**). Furthermore, we compared our two sedimentary records with the only two reported ²³³U records resolved from a peat core (Black forest, Germany) and a coral core (Kume Island, Japan)¹⁴ (**Figure 3**). The peat core only received global fallout signal, and the coral core was affected by both global fallout and close-in fallout from Pacific Proving Ground (PPG) (**Table S1**).¹⁴ With dating uncertainties, elevated ²³³U/²³⁸U atomic ratios appear in all available records in

the mid-to-late 1950s (blue bar in **Figure 2**), which indicates a remarkable global atmospheric deposition of ^{233}U .

A previous study proposed two potential sources for global-fallout-derived ^{233}U .¹⁴ The first one is the nuclear weapon tests directly using ^{233}U as fissile material and releasing unfissioned ^{233}U into the atmosphere.¹⁴ To the best of our knowledge, one experimental device using a composite pit of ^{239}Pu and ^{233}U was donated by the United States in 1955 at the Nevada Test Site (**Operation Teapot "MET"** test, 22kt).⁴⁸ The former Soviet Union's two-stage hydrogen bomb tested in 1955 at the Semipalatinsk Test Site ("RDS-37", 3Mt) also utilized ^{235}U and ^{233}U as fuel in the fissile core.⁴⁹ Considering a much higher yield, the "RDS-37" test likely ejected more ^{233}U debris into the stratosphere and thereby resulted in a global fallout.⁵⁰ The second source is the thermonuclear weapon tests using enriched U (so-called oralloy) as tamper material and producing ^{233}U via the fast neutron reaction $^{235}\text{U}(n,3n)^{233}\text{U}$.¹⁴ According to the disclosed information, the first thermonuclear weapon test with an oralloy tamper is the Operation Castle "Nectar" test conducted by the United States at the PPG in 1954.¹⁴ In addition, several thermonuclear weapon tests of the Operation Hardtack I with Mt yields implemented at the PPG in 1958 were also suspected to use oralloy tampers, as indicated by elevated $^{236}\text{U}/^{239}\text{Pu}$ atomic ratios found in other corals at Enewetak Atoll.¹⁴

The universe ^{233}U signal in the three locations across Europe to Asia is likely attributed to the detonation of two ^{233}U devices in 1955, especially the former Soviet Union's "RDS-37" test. The Baltic Sea sediment cores have much higher maximum $^{233}\text{U}/^{236}\text{U}$ atomic ratios ($(6.42 - 15.3) \times 10^{-2}$) than the peat and coral cores, suggesting that the Baltic Sea is closer to the test site that is most likely the Semipalatinsk Test Site for "RDS-37" test. Unfortunately, the resolutions in the peat core and the sediment cores are rather poor in the late 1950s and early 1960s to provide a further evidence on whether the United States' Operation Hardtack I tests released significant amounts of ^{233}U or not.

Based on the areal cumulative inventories of ^{233}U in sediment and peat cores, the representative areal inventory of ^{233}U from the direct deposition of global fallout should be at the level of $10^{10} - 10^{11}$ atom/m² in the Northern European region (see Supplementary Discussions in Supporting Information). The total release of ^{233}U from the nuclear weapons testing is roughly estimated to be 7 - 15 kg, assuming an areal ^{233}U inventory of $(5 - 12) \times 10^{10}$ atom/m² in the Northern Hemisphere and a one-third level in the Southern Hemisphere according to the investigations on the global-fallout-derived ^{90}Sr .⁵⁰ This estimation is at the same order of the calculation results (12 - 29 kg) based on the estimated global-fallout-derived ^{236}U inventory (900 - 2100 kg) and representative $^{233}\text{U}/^{236}\text{U}$ atomic ratios for global fallout ($(1.40 \pm 0.15) \times 10^{-2}$).

Quantification of ^{236}U from Different Nuclear Activities.

The Gotland Basin and Landsort Deep sediments have similar areal cumulative inventories of ^{236}U , which are estimated to be $(3.53 \pm 0.19) \times 10^{13}$ atom/m² and $(3.16 \pm 0.13) \times 10^{13}$ atom/m², respectively. Except for a pronounced peak in ~1986 only observed in the Landsort Deep sediment core, the depth profiles of $^{236}\text{U}/^{238}\text{U}$ atomic ratios in both sediment cores are also very consistent, including an increase before the late 1970s, a relatively constant level during the 1980s, and a gentle decline after the early 1990s (**Figure 3**).

As the reducing bottom water conditions are favorable for the sedimentation and preservation of U isotopes, a total inventory of 607 - 679 g ^{236}U can be roughly estimated in the Baltic sediments assuming a hypoxic area of ~ 49,000 km² (avg. during 1961-2000)² and similar areal cumulative ^{236}U inventory in the hypoxic area to the Gotland Basin and Landsort Deep. However, the deposition of ^{236}U in the oxygenated area of the Baltic Sea was not considered in this estimation due to lack of observation data.

To clarify the sources of ^{236}U to the Baltic Sea, we compared the temporal distribution of $^{233}\text{U}/^{236}\text{U}$ atomic ratios in the sediment, peat, and core cores (**Figure 3**).¹⁴ It should be noted that the $^{233}\text{U}/^{236}\text{U}$ atomic ratios in various records have different enlightenments (see Supplementary Discussions in Supporting Information). Before the mid-1960s, an earlier intensive deposition of ^{233}U than ^{236}U leads to higher $^{233}\text{U}/^{236}\text{U}$ atomic ratios than the modern integrated global fallout signal ($(1.40 \pm 0.15) \times 10^{-2}$) in the Baltic sediment cores, which is consistent with the peat core record. In the mid-to-late 1960s, $^{233}\text{U}/^{236}\text{U}$ atomic ratios approach to 1.4×10^{-2} in all settings (green bar in **Figure 3**). The record of the peat core indicates that more than 90% of ^{233}U and 80% of ^{236}U have deposited by the year of 1970 due to the partial nuclear test ban treaty in 1963. Therefore, the main source term of ^{236}U in the Baltic sediments before the late 1960s should be identical to that in the peat core, i.e., global fallouts. Since 1970, $^{233}\text{U}/^{236}\text{U}$ atomic ratios in the peat and coral cores remain constant at 1.4×10^{-2} , suggesting that the ratio of ^{233}U and ^{236}U on the earth's surface environment reach equilibrium. While, $^{233}\text{U}/^{236}\text{U}$ atomic ratios start to fall below 1.4×10^{-2} in the Baltic sediments, reflecting the appearance of reactor-derived ^{236}U input(s) (e.g., from reprocessing plants and other local facilities) to the Baltic Sea. The remarkable drop of $^{233}\text{U}/^{236}\text{U}$ atomic ratios in ~1986 in the Landsort Deep composite core is attributed to the reactor-derived ^{236}U from the Chernobyl accident (26th April, 1986), which is supported by the pronounced ^{137}Cs signal in the same sediment interval (**Figure 3**).

Using $^{233}\text{U}/^{236}\text{U}$ as signature, a two-endmember mixing model is adopted to calculate the proportions of global-fallout-derived and reactor-derived ^{236}U (^{238}U) in two sediment cores (see Calculations in *S/Appendix*), and the results are shown in **Figure 4**. The global-fallout-derived and reactor-derived ^{236}U account for $(43.3 \pm 2.8)\%$ and $(56.7 \pm 8.0)\%$ of total ^{236}U in the Gotland Basin sediment core, respectively. While the global-fallout-derived, reactor-derived (excluding Chernobyl accident), and Chernobyl-derived ^{236}U contribute $(50.5 \pm 2.1)\%$, $(48.6 \pm 5.3)\%$, and $(0.9 \pm 0.2)\%$ of total ^{236}U to the Landsort Deep composite core, respectively. In general, global fallout and discharges of civil nuclear industry (i.e.

reprocessing plants and local nuclear facilities) have comparable ^{236}U inputs to the Baltic Sea, whereas contribution from the Chernobyl accident is negligible.

Input History of ^{236}U to the Baltic Sea.

The potential ^{236}U inputs to the Baltic Sea include: (i) global-fallout-related inputs, comprising the direct atmospheric deposition, and indirect inputs from the North Sea and North Atlantic via Baltic inflows and from the catchment via river run-off; and (ii) reactor-related inputs, including the discharges from nuclear reprocessing plants followed by transport to the Baltic through oceanic currents, releases from local nuclear facilities, and regional fallout from the Chernobyl accidents (**Figure 1**).

i) Global fallout inputs. Global-fallout-derived $^{236}\text{U}/^{238}\text{U}$ atomic ratios in Baltic sediment cores represent an integration of directly deposited particulate fallout and scavenged soluble global-fallout-derived ^{236}U from the water column. As more than 95% of ^{236}U fallout have deposited by 1980 according to the record of the peat core, the ^{236}U in the Baltic sediments mainly originates from the scavenging processes since 1980 and sedimentary global-fallout-derived $^{236}\text{U}/^{238}\text{U}$ atomic ratios should mainly reveal the historical levels in the deep waters (where U is scavenged). The decreasing trends in the Baltic sediments since 1980 is consistent with the reported records of coral cores from the Caribbean Sea, Japan Sea, and the Northwest Pacific Ocean (**Figure S9**).^{18,27,28} We calculated the effective half-life of global-fallout-derived ^{236}U based on the observation data (**see Details for the Calculations in Supporting Information**), which is estimated to be 29 - 54 years in these seas with different hydrographic and physio-chemical conditions. The effective half-life of ^{236}U is much shorter than its radioactive half-life (23.4 Myr), and this should be considered in its future tracer studies.

The resolved global-fallout-derived $^{236}\text{U}/^{238}\text{U}$ atomic ratios in the Baltic Sea are about one order of magnitude higher than other aforementioned seas (**Figure S9**). Assuming a ^{238}U concentration of 1.2 $\mu\text{g}/\text{kg}$ in the bottom waters of the Gotland Basin and Landsort Deep according to their bottom average salinity,⁵¹ the global-fallout-derived ^{236}U concentration is estimated to be $\sim 1.8 \times 10^7$ atoms/kg in the 2010s. This is comparable with the observation results of the surface water in the central Baltic Sea in 2015 ($(1.6 - 1.8) \times 10^7$ atoms/kg)⁸, and about two times higher than the representative level in the open sea as well as the simulated level in the North Sea ($\sim 8 \times 10^6$ atoms/kg)²³. A potential reason is that the long residence time of water in the Baltic Sea (~ 30 years)⁴ is favor to the preservation of "aged" waters with higher global-fallout-derived ^{236}U concentrations e.g. from the North Sea and/or river runoff.

ii) Chernobyl accident input. The notable $^{236}\text{U}/^{238}\text{U}$ peak in Landsort Deep composite core with no significant change in the $^{233}\text{U}/^{238}\text{U}$ atomic ratios indicates a pure ^{236}U input in ~ 1986 (**Figure 3**). In contrast, no $^{236}\text{U}/^{238}\text{U}$ peak is observed in the Gotland Basin sediment core in ~ 1986 , even though clear Chernobyl ^{137}Cs and ^{241}Am signals show up (**Figure 3**). One possible explanation is that the Landsort Deep is closer to the regions that was highly contaminated by the Chernobyl fallout, including the Bothnian Sea and the central Sweden.⁵² Another reason is that Chernobyl-derived ^{236}U might deposit to

the Baltic sediments as "hot particles". Different from the ^{137}Cs activities that decline gradually after 1986, the $^{236}\text{U}/^{238}\text{U}$ atomic ratios in the Landsort Deep composite core quickly decrease to the pre-Chernobyl level, as also seen in the ^{241}Am peak of the Gotland Basin sediment core. Considering that Am is highly particle-reactive and less mobile than Cs, the input of the Chernobyl-derived ^{236}U was likely a pulse atmospheric deposition as particulate-associated forms as well.

iii) Civil nuclear industry inputs. Excluding the Chernobyl-derived ^{236}U input, the temporal distribution of reactor-derived $^{236}\text{U}/^{238}\text{U}$ atomic ratios in the Baltic Sea sediment cores mainly reveal the input history of reactor-derived ^{236}U from civil nuclear industry (**Figure 4**), including the liquid discharges from the two major European nuclear reprocessing plants and local nuclear facilities ⁸.

As dominating regional sources, the reprocessing plants at Sellafield and La Hague were estimated to release >237 kg and ~25 kg of ^{236}U ,¹⁹ and the reprocessing-derived ^{236}U are transported to the North Sea via the Scottish Coastal Current and English Channel Current.⁵³ As previous model calculations indicated that 1% of the reprocessing discharges can reach the Baltic Sea,⁵² the total inputs of reprocessing-derived ^{236}U to the Baltic Sea can be roughly estimated as 2.6 kg. The decreasing of reactor-derived $^{236}\text{U}/^{238}\text{U}$ atomic ratios in the Baltic sediments since the mid-1980s is also consistent with the declined discharges of reprocessing-derived ^{236}U discharges in the recent decades.¹⁹ For comparison, the total deposition of global-fallout-derived ^{236}U on the Baltic Sea is estimated to be 1.5 kg (ignoring the indirect inputs).⁸ The above rough estimations indicate that the inputs of reprocessing-derived and global-fallout-derived ^{236}U seem to be at the same magnitude, which agree well with our sediment observation data.

Except for nuclear reprocessing plants, our recent research estimated that additional 200 ± 47 g of reactor-derived ^{236}U was released to the Baltic Sea by an unknown source.⁸ Excluding the Chernobyl accident, the most possible candidates are the local nuclear facilities, including nuclear power plants in Sweden (Barsebäck, Ringhals, Oskarshamn, and Forsmark), Finland (Olkiluoto), Russia (Leningrad and Kaliningrad) and Germany (Greifswald), some research facilities (Risø and Studsvik) and the nuclear fuel fabrication facility (Westinghouse) in Sweden. The only documented ^{236}U sources are 0.44 g of aquatic discharge and 0.016 g of airborne emission from Westinghouse during 2002-2017,²⁶ which are negligible compared with the above-mentioned additional reactor-derived ^{236}U input. No significantly high levels of ^{236}U have been reported in the surrounding environment of other nuclear facilities, except for the nuclear research company Studsvik, which has been in operation since the 1950s and reported to dump 64 tons of radioactive waste into the coastal area nearby during 1959-1961.⁵⁴ However, no detectable reactor-derived ^{236}U signal is observed in the Baltic Sea sediments cores around 1960. Further investigation is still needed to uncover the source of additional reactor-derived ^{236}U . We should be aware that these additional reactor-derived ^{236}U only contribute a small fraction to the ^{236}U budget of the Baltic Sea.⁸ For instance, even if 20% of the unknown ^{236}U source (~ 40 g) is scavenged to the sediments, they are still minor compared with the present total sedimentary reactor-derived ^{236}U (295 - 385 g).

Associated Content

Supporting Information.

Details for the Analytical Methods, including: dating for sediment cores; determination of Al, Hg, Mn, U contents, $^{206}/^{207}\text{Pb}$ ratios and TOC in the sediments; determination of dissolved U, particulate U, and sulfide in seawater and porewater; determination of $^{236}\text{U}/^{238}\text{U}$ and $^{233}\text{U}/^{238}\text{U}$ and $^{233}\text{U}/^{236}\text{U}$ atomic ratios in the sediments; background control measures for ^{236}U and ^{233}U analyses; and determination of ^{137}Cs and ^{241}Am activities in the sediment. Details for the calculations, including: quantification of anthropogenic ^{236}U from different sources and calculation of effective half-life of global-fallout-derived ^{236}U . Supplementary discussions for scavenging processes of U, areal inventory of ^{233}U from the direct deposition of global fallout, and interpretations behind the records of peat, coral, and sediment cores. Supplementary figures, including: the depth profiles in the sediment core 7-MUC4; the age-depth relation for the core 7-MUC4; instrumental time series of $\text{O}_2/\text{H}_2\text{S}$ in the Landsort Deep and the depth profiles in the sediment core 36-MUC3; the combined age-depth relation for the core 36-MUC3; transfer of the age model from the core 36-MUC3 to the core 11-10MUC2; the resulting age-depth relation for the composite core 11-10MUC2/36-MUC3; comparison between instrumental time series of $\text{O}_2/\text{H}_2\text{S}$ in the Landsort Deep and the depth profile of Mn contents in the composite core 11-10MUC2/36-MUC3; comparison of water-column time series and the sedimentary record, as well as water column and pore water profiles from the Landsort Deep; and contemporary comparison of global-fallout-derived (GF-derived) $^{236}\text{U}/^{238}\text{U}$ atomic ratios. Supplementary tables, including: overview of the resolved records of ^{236}U and ^{233}U in the published and present studies; results for a leaching experiment of the Baltic Sea sediments; measurement results of U, Mn, Al, TOC contents, and mass ratio of U/Al in the core 7-MUC4 and the core 11-10MUC2/36-MUC3; and measurement results of $^{236}\text{U}/^{238}\text{U}$, $^{233}\text{U}/^{238}\text{U}$, and $^{233}\text{U}/^{236}\text{U}$ atomic ratios, ^{137}Cs activities, ^{241}Am activities, and calculation results of global-fallout-derived and reactor-derived $^{236}\text{U}/^{238}\text{U}$ atomic ratios in the core 7-MUC4 and the core 11-10MUC2/36-MUC3.

Declarations

Author Contributions

M.L. performed sample analysis and wrote the manuscript; J.Q. designed and coordinated the research; X.H. assisted with supervision. O.D. provided samples; O.D., P.S., K.H., R.G., and L.Z. assisted with sample analysis; All authors contributed to reviewing and editing.

Notes

The authors declare no competing interests.

Acknowledgment

We wish to thank all colleagues in DTU-ENV for the support on this research, the crews and captains of RVs Elisabeth Mann Borgese and Meteor for technical support during field work, and Anne Köhler for lab assistance at IOW. The work at IOW was funded by the Leibniz Association, through grant SAW-2017-IOW-2 649 (BaltRap).

References

- (1) Mohrholz, V.; Naumann, M.; Nausch, G.; Krüger, S.; Gräwe, U. Fresh Oxygen for the Baltic Sea – An Exceptional Saline Inflow after a Decade of Stagnation. *Journal of Marine Systems* **2015**, *148*, 152–166. <https://doi.org/10.1016/j.jmarsys.2015.03.005>.
- (2) Conley, D. J.; Björck, S.; Bonsdorff, E.; Carstensen, J.; Destouni, G.; Gustafsson, B. G.; Hietanen, S.; Kortekaas, M.; Kuosa, H.; Markus Meier, H. E.; Müller-Karulis, B.; Nordberg, K.; Norkko, A.; Nürnberg, G.; Pitkänen, H.; Rabalais, N. N.; Rosenberg, R.; Savchuk, O. P.; Slomp, C. P.; Voss, M.; Wulff, F.; Zillén, L. Hypoxia-Related Processes in the Baltic Sea. *Environ. Sci. Technol.* **2009**, *43* (10), 3412–3420. <https://doi.org/10.1021/es802762a>.
- (3) Markus Meier, H. E. Modeling the Pathways and Ages of Inflowing Salt- and Freshwater in the Baltic Sea. *Estuarine, Coastal and Shelf Science* **2007**, *74* (4), 610–627. <https://doi.org/10.1016/j.ecss.2007.05.019>.
- (4) Franck, H.; Matthaus, W.; Sammler, R. Major Inflows of Saline Water into the Baltic Sea during the Present Century. *Gerlands Beitrage Zur Geophysik* **1987**, *96* (6).
- (5) Andersen, J. H.; Carstensen, J.; Conley, D. J.; Dromph, K.; Fleming-Lehtinen, V.; Gustafsson, B. G.; Josefson, A. B.; Norkko, A.; Villnäs, A.; Murray, C. Long-Term Temporal and Spatial Trends in Eutrophication Status of the Baltic Sea: Eutrophication in the Baltic Sea. *Biol Rev* **2017**, *92* (1), 135–149. <https://doi.org/10.1111/brv.12221>.
- (6) Meier, H. E. M.; Eilola, K.; Almroth-Rosell, E.; Schimanke, S.; Kniebusch, M.; Höglund, A.; Pemberton, P.; Liu, Y.; Väli, G.; Saraiva, S. Disentangling the Impact of Nutrient Load and Climate Changes on Baltic Sea Hypoxia and Eutrophication since 1850. *Clim Dyn* **2019**, *53* (1–2), 1145–1166. <https://doi.org/10.1007/s00382-018-4296-y>.
- (7) Carstensen, J.; Andersen, J. H.; Gustafsson, B. G.; Conley, D. J. Deoxygenation of the Baltic Sea during the Last Century. *Proceedings of the National Academy of Sciences* **2014**, *111* (15), 5628–5633. <https://doi.org/10.1073/pnas.1323156111>.
- (8) Qiao, J.; Zhang, H.; Steier, P.; Hain, K.; Hou, X.; Vartti, V.-P.; Henderson, G. M.; Eriksson, M.; Aldahan, A.; Possnert, G.; Golser, R. An Unknown Source of Reactor Radionuclides in the Baltic Sea Revealed by Multi-Isotope Fingerprints. *Nat Commun* **2021**, *12* (1), 823. <https://doi.org/10.1038/s41467-021-21059-w>.

- (9) Qiao, J.; Steier, P.; Nielsen, S.; Hou, X.; Roos, P.; Golser, R. Anthropogenic ^{236}U in Danish Seawater: Global Fallout versus Reprocessing Discharge. *Environ. Sci. Technol.* **2017**, *51* (12), 6867–6876. <https://doi.org/10.1021/acs.est.7b00504>.
- (10) Hou, X. L.; Dahlgaard, H.; Nielsen, S. P.; Kucera, J. Level and Origin of Iodine-129 in the Baltic Sea. *Journal of Environmental Radioactivity* **2002**, *61* (3), 331–343. [https://doi.org/10.1016/S0265-931X\(01\)00143-6](https://doi.org/10.1016/S0265-931X(01)00143-6).
- (11) Qiao, J.; Andersson, K.; Nielsen, S. A 40-Year Marine Record of ^{137}Cs and ^{99}Tc Transported into the Danish Straits: Significance for Oceanic Tracer Studies. *Chemosphere* **2020**, *244*, 125595. <https://doi.org/10.1016/j.chemosphere.2019.125595>.
- (12) Casacuberta, N.; Christl, M.; Lachner, J.; van der Loeff, M. R.; Masqué, P.; Synal, H.-A. A First Transect of ^{236}U in the North Atlantic Ocean. *Geochimica et Cosmochimica Acta* **2014**, *133*, 34–46. <https://doi.org/10.1016/j.gca.2014.02.012>.
- (13) Swanson, V. E.; Swanson, V. E. *Geology and Geochemistry of Uranium in Marine Black Shales: A Review*, US Government Printing Office Washington, DC, 1961.
- (14) Hain, K.; Steier, P.; Froehlich, M. B.; Golser, R.; Hou, X.; Lachner, J.; Nomura, T.; Qiao, J.; Quinto, F.; Sakaguchi, A. $^{233}\text{U}/^{236}\text{U}$ Signature Allows to Distinguish Environmental Emissions of Civil Nuclear Industry from Weapons Fallout. *Nat Commun* **2020**, *11* (1), 1275. <https://doi.org/10.1038/s41467-020-15008-2>.
- (15) Dunk, R. M.; Mills, R. A.; Jenkins, W. J. A Reevaluation of the Oceanic Uranium Budget for the Holocene. *Chemical Geology* **2002**, *190* (1–4), 45–67. [https://doi.org/10.1016/S0009-2541\(02\)00110-9](https://doi.org/10.1016/S0009-2541(02)00110-9).
- (16) Sakaguchi, A.; Kawai, K.; Steier, P.; Quinto, F.; Mino, K.; Tomita, J.; Hoshi, M.; Whitehead, N.; Yamamoto, M. First Results on ^{236}U Levels in Global Fallout. *Science of The Total Environment* **2009**, *407* (14), 4238–4242. <https://doi.org/10.1016/j.scitotenv.2009.01.058>.
- (17) Christl, M.; Lachner, J.; Vockenhuber, C.; Lechtenfeld, O.; Stimac, I.; van der Loeff, M. R.; Synal, H.-A. A Depth Profile of Uranium-236 in the Atlantic Ocean. *Geochimica et Cosmochimica Acta* **2012**, *77*, 98–107. <https://doi.org/10.1016/j.gca.2011.11.009>.
- (18) Winkler, S. R.; Steier, P.; Carilli, J. Bomb Fall-out ^{236}U as a Global Oceanic Tracer Using an Annually Resolved Coral Core. *Earth and Planetary Science Letters* **2012**, *359–360*, 124–130. <https://doi.org/10.1016/j.epsl.2012.10.004>.
- (19) Castrillejo, M.; Witbaard, R.; Casacuberta, N.; Richardson, C. A.; Dekker, R.; Synal, H.-A.; Christl, M. Unravelling 5 Decades of Anthropogenic ^{236}U Discharge from Nuclear Reprocessing Plants. *Science of The Total Environment* **2020**, *717*, 137094. <https://doi.org/10.1016/j.scitotenv.2020.137094>.

- (20) Casacuberta, N. First ^{236}U Data from the Arctic Ocean and Use of $^{236}\text{U}/^{238}\text{U}$ and $^{129}\text{I}/^{236}\text{U}$ as a New Dual Tracer. *Earth and Planetary Science Letters* **2016**, 8.
- (21) Casacuberta, N.; Christl, M.; Vockenhuber, C.; Wefing, A.-M.; Wacker, L.; Masqué, P.; Synal, H.-A.; Rutgers van der Loeff, M. Tracing the Three Atlantic Branches Entering the Arctic Ocean With ^{129}I and ^{236}U . *J. Geophys. Res. Oceans* **2018**, 123 (9), 6909–6921. <https://doi.org/10.1029/2018JC014168>.
- (22) Wefing, A.-M.; Casacuberta, N.; Christl, M.; Gruber, N.; Smith, J. N. Circulation Timescales of Atlantic Waters in the Arctic Ocean Determined from Anthropogenic Radionuclides. *Ocean Science Discussions* **2020**, 2020, 1–29. <https://doi.org/10.5194/os-2020-82>.
- (23) Christl, M.; Casacuberta, N.; Vockenhuber, C.; Elsasser, C.; Bailly du Bois, P.; Herrmann, J.; Synal, H.-A. Reconstruction of the ^{236}U Input Function for the Northeast Atlantic Ocean: Implications for $^{129}\text{I}/^{236}\text{U}$ and $^{236}\text{U}/^{238}\text{U}$ -Based Tracer Ages. *Journal of Geophysical Research* **2015**, 18.
- (24) Qiao, J.; Hain, K.; Steier, P. First Dataset of ^{236}U and ^{233}U around the Greenland Coast: A 5-Year Snapshot (2012–2016). *Chemosphere* **2020**, 257, 127185. <https://doi.org/10.1016/j.chemosphere.2020.127185>.
- (25) Naegeli, R. E. *Calculation of the Radionuclides in PWR Spent Fuel Samples for SFR Experiment Planning*; SAND2004-2757, 919122; 2004; pp SAND2004-2757, 919122. <https://doi.org/10.2172/919122>.
- (26) HELCOM. HELCOM MORS Discharge database <https://helcom.fi/%20baltic-sea-trends/data-maps/databases/> (accessed May 1, 2020).
- (27) Nomura, T.; Sakaguchi, A.; Steier, P.; Eigl, R.; Yamakawa, A.; Watanabe, T.; Sasaki, K.; Watanabe, T.; Golser, R.; Takahashi, Y.; Yamano, H. Reconstruction of the Temporal Distribution of $^{236}\text{U}/^{238}\text{U}$ in the Northwest Pacific Ocean Using a Coral Core Sample from the Kuroshio Current Area. *Marine Chemistry* **2017**, 190, 28–34. <https://doi.org/10.1016/j.marchem.2016.12.008>.
- (28) Sakaguchi, A.; Nomura, T.; Steier, P.; Golser, R.; Sasaki, K.; Watanabe, T.; Nakakuki, T.; Takahashi, Y.; Yamano, H. Temporal and Vertical Distributions of Anthropogenic ^{236}U in the J Apan S Ea Using a Coral Core and Seawater Samples. *J. Geophys. Res. Oceans* **2016**, 121 (1), 4–13. <https://doi.org/10.1002/2015JC011109>.
- (29) Seeberg-Elverfeldt, J.; Schlüter, M.; Feseker, T.; Kölling, M. Rhizon Sampling of Porewaters near the Sediment-Water Interface of Aquatic Systems: Rhizon Porewater Sampling. *Limnol. Oceanogr. Methods* **2005**, 3 (8), 361–371. <https://doi.org/10.4319/lom.2005.3.361>.
- (30) Dellwig, O.; Wegwerth, A.; Schnetger, B.; Schulz, H.; Arz, H. W. Dissimilar Behaviors of the Geochemical Twins W and Mo in Hypoxic-Euxinic Marine Basins. *Earth-Science Reviews* **2019**, 193, 1–23. <https://doi.org/10.1016/j.earscirev.2019.03.017>.

- (31) Cline, J. Spectrophotometric Determination of Hydrogen Sulfide in Natural Waters. *Limnology and Oceanography* **1969**, *14* (3).
- (32) Qiao, J.; Hou, X.; Steier, P.; Nielsen, S.; Golser, R. Method for ^{236}U Determination in Seawater Using Flow Injection Extraction Chromatography and Accelerator Mass Spectrometry. *Anal. Chem.* **2015**, *87* (14), 7411–7417. <https://doi.org/10.1021/acs.analchem.5b01608>.
- (33) Lin, M.; Qiao, J.; Hou, X.; Golser, R.; Hain, K.; Steier, P. On the Quality Control for the Determination of Ultratrace-Level ^{236}U and ^{233}U in Environmental Samples by Accelerator Mass Spectrometry. *Anal. Chem.* **2021**, *acs.analchem.0c03623*. <https://doi.org/10.1021/acs.analchem.0c03623>.
- (34) Lee, S. H.; Povinec, P. P.; Wyse, E.; Hotchkis, M. A. C. Ultra-Low-Level Determination of ^{236}U in IAEA Marine Reference Materials by ICPMS and AMS. *Applied Radiation and Isotopes* **2008**, *66* (6–7), 823–828. <https://doi.org/10.1016/j.apradiso.2008.02.020>.
- (35) Dellwig, O.; Schnetger, B.; Meyer, D.; Pollehne, F.; Häusler, K.; Arz, H. W. Impact of the Major Baltic Inflow in 2014 on Manganese Cycling in the Gotland Deep (Baltic Sea). *Front. Mar. Sci.* **2018**, *5*, 248. <https://doi.org/10.3389/fmars.2018.00248>.
- (36) Häusler, K.; Dellwig, O.; Schnetger, B.; Feldens, P.; Leipe, T.; Moros, M.; Pollehne, F.; Schönke, M.; Wegwerth, A.; Arz, H. W. Massive Mn Carbonate Formation in the Landsort Deep (Baltic Sea): Hydrographic Conditions, Temporal Succession, and Mn Budget Calculations. *Marine Geology* **2018**, *395*, 260–270. <https://doi.org/10.1016/j.margeo.2017.10.010>.
- (37) Moros, M.; Andersen, T. J.; Schulz-Bull, D.; Häusler, K.; Bunke, D.; Snowball, I.; Kotilainen, A.; Zillén, L.; Jensen, J. B.; Kabel, K.; Hand, I.; Leipe, T.; Lougheed, B. C.; Wagner, B.; Arz, H. W. Towards an Event Stratigraphy for Baltic Sea Sediments Deposited since AD 1900: Approaches and Challenges. *Boreas* **2017**, *46* (1), 129–142. <https://doi.org/10.1111/bor.12193>.
- (38) Brumsack, H.-J. The Trace Metal Content of Recent Organic Carbon-Rich Sediments: Implications for Cretaceous Black Shale Formation. *Palaeogeography, Palaeoclimatology, Palaeoecology* **2006**, *232* (2–4), 344–361. <https://doi.org/10.1016/j.palaeo.2005.05.011>.
- (39) Bröske, A.; Weyer, S.; Zhao, M.-Y.; Planavsky, N. J.; Wegwerth, A.; Neubert, N.; Dellwig, O.; Lau, K. V.; Lyons, T. W. Correlated Molybdenum and Uranium Isotope Signatures in Modern Anoxic Sediments: Implications for Their Use as Paleo-Redox Proxy. *Geochimica et Cosmochimica Acta* **2020**, *270*, 449–474. <https://doi.org/10.1016/j.gca.2019.11.031>.
- (40) Langmuir, D. Uranium Solution-Mineral Equilibria at Low Temperatures with Applications to Sedimentary Ore Deposits. *Geochimica et Cosmochimica Acta* **1978**, *42* (6), 547–569.
- (41) Anderson, R. F.; Fleisher, M. Q.; LeHuray, A. P. Concentration, Oxidation State, and Particulate Flux of Uranium in the Black Sea. *Geochimica et Cosmochimica Acta* **1989**, *53* (9), 2215–2224.

[https://doi.org/10.1016/0016-7037\(89\)90345-1](https://doi.org/10.1016/0016-7037(89)90345-1).

- (42) Barnes, C.; Cochran, J. Uranium Removal in Oceanic Sediments and the Oceanic U Balance. *Earth and Planetary Science Letters* **1990**, *97* (1–2), 94–101.
- (43) Klinkhammer, G. P.; Palmer, M. R. Uranium in the Oceans: Where It Goes and Why. *Geochimica et Cosmochimica Acta* **1991**, *55* (7), 1799–1806. [https://doi.org/10.1016/0016-7037\(91\)90024-Y](https://doi.org/10.1016/0016-7037(91)90024-Y).
- (44) Lovley, D. R.; Phillips, E. J. P.; Gorby, Y. A.; Landa, E. R. Microbial Reduction of Uranium. *Nature* **1991**, *350* (6317), 413–416. <https://doi.org/10.1038/350413a0>.
- (45) Diaz, R. J.; Rosenberg, R. Spreading Dead Zones and Consequences for Marine Ecosystems. *Science* **2008**, *321* (5891), 926–929. <https://doi.org/10.1126/science.1156401>.
- (46) Rudnick, R. L.; Gao, S. Composition of the Continental Crust. In *Treatise on Geochemistry*; Elsevier, 2014; pp 1–51. <https://doi.org/10.1016/B978-0-08-095975-7.00301-6>.
- (47) Steier, P.; Bichler, M.; Keith Fifield, L.; Golser, R.; Kutschera, W.; Priller, A.; Quinto, F.; Richter, S.; Srnčik, M.; Terrasi, P.; Wacker, L.; Wallner, A.; Wallner, G.; Wilcken, K. M.; Maria Wild, E. Natural and Anthropogenic ^{236}U in Environmental Samples. *Nuclear Instruments and Methods in Physics Research Section B: Beam Interactions with Materials and Atoms* **2008**, *266* (10), 2246–2250. <https://doi.org/10.1016/j.nimb.2008.03.002>.
- (48) Alvarez, R. Managing the Uranium-233 Stockpile of the United States. *Science & Global Security* **2013**, *21* (1), 53–69. <https://doi.org/10.1080/08929882.2013.754311>.
- (49) Holloway, D. Research Note: Soviet Thermonuclear Development. *International Security* **1979**, *4* (3), 192–197.
- (50) *Sources and Effects of Ionizing Radiation: United Nations Scientific Committee on the Effects of Atomic Radiation: UNSCEAR 2000 Report to the General Assembly, with Scientific Annexes*; United Nations, Ed.; United Nations: New York, 2000.
- (51) ICES. ICES Dataset on Oceanography <https://ices.dk/data/dataset-collections/Pages/default.aspx> (accessed May 1, 2020).
- (52) Nielsen, S. P.; Lüning, M.; Illus, E.; Outola, I.; Ikäheimonen, T.; Mattila, J.; Herrmann, J.; Kanisch, G.; Osvath, I. Baltic Sea: Radionuclides. In *Encyclopedia of Inorganic Chemistry*; King, R. B., Crabtree, R. H., Lukehart, C. M., Atwood, D. A., Scott, R. A., Eds.; John Wiley & Sons, Ltd: Chichester, UK, 2010; p ia760. <https://doi.org/10.1002/0470862106.ia760>.
- (53) Christl, M.; Casacuberta, N.; Lachner, J.; Herrmann, J.; Synal, H.-A. Anthropogenic ^{236}U in the North Sea – A Closer Look into a Source Region. *Environ. Sci. Technol.* **2017**, *51* (21), 12146–12153. <https://doi.org/10.1021/acs.est.7b03168>.

Figures

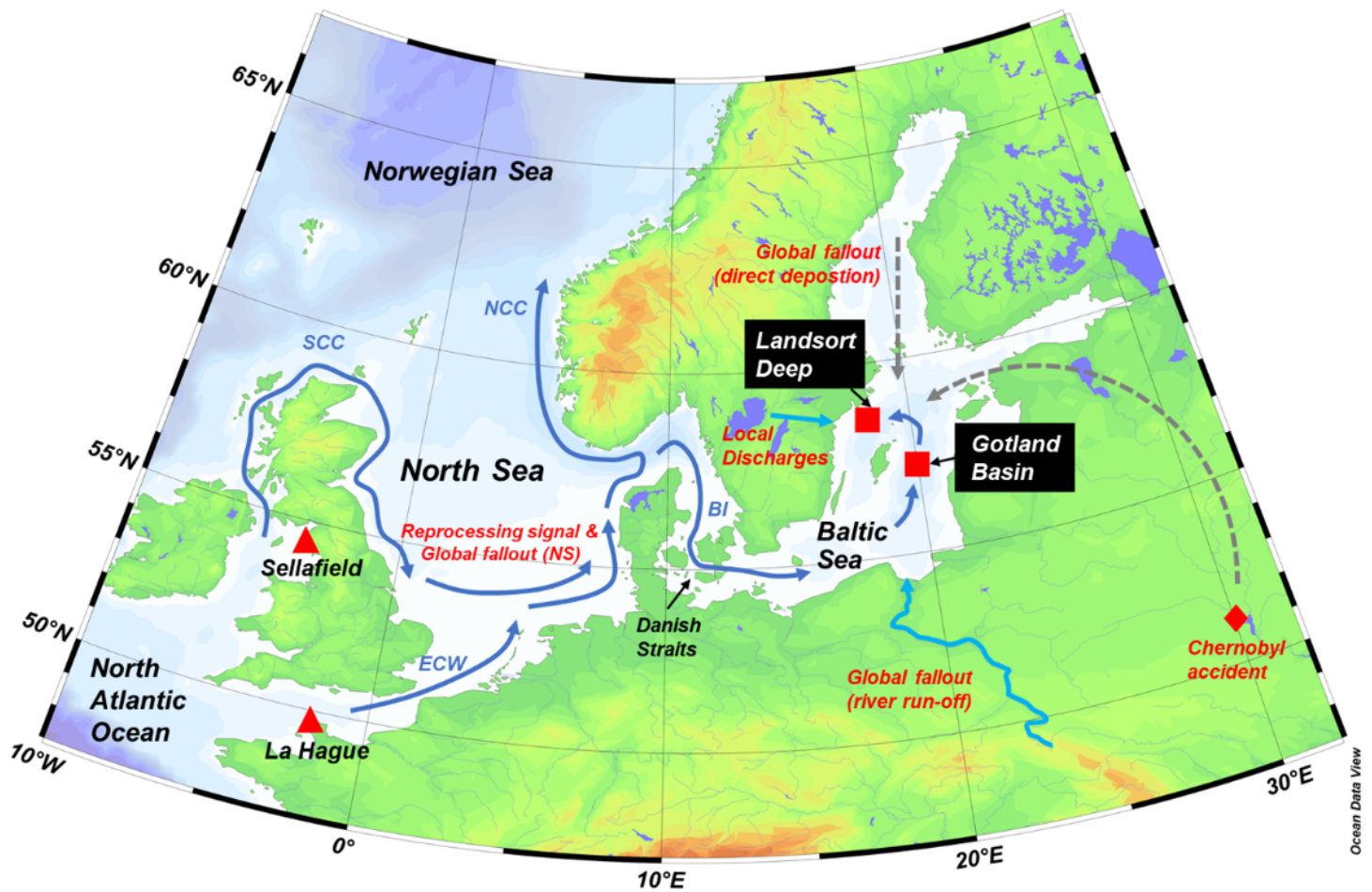


Figure 1

Schematic illustration of sampling sites and ^{236}U and ^{233}U inputs to the Baltic Sea. The red square refers to the sampling locations of the sediment cores in this work; the dark blue arrows represent the major oceanic currents in North Sea - Baltic Sea region (ECW: English Channel waters; SCC: Scottish coastal current; NCC: Norwegian coastal current; BI: Baltic inflows, NS: North Sea); light blue arrows represent river run-off and potential liquid discharges from local facilities; grey arrows represent the atmospheric deposition from global fallout and the Chernobyl accident.

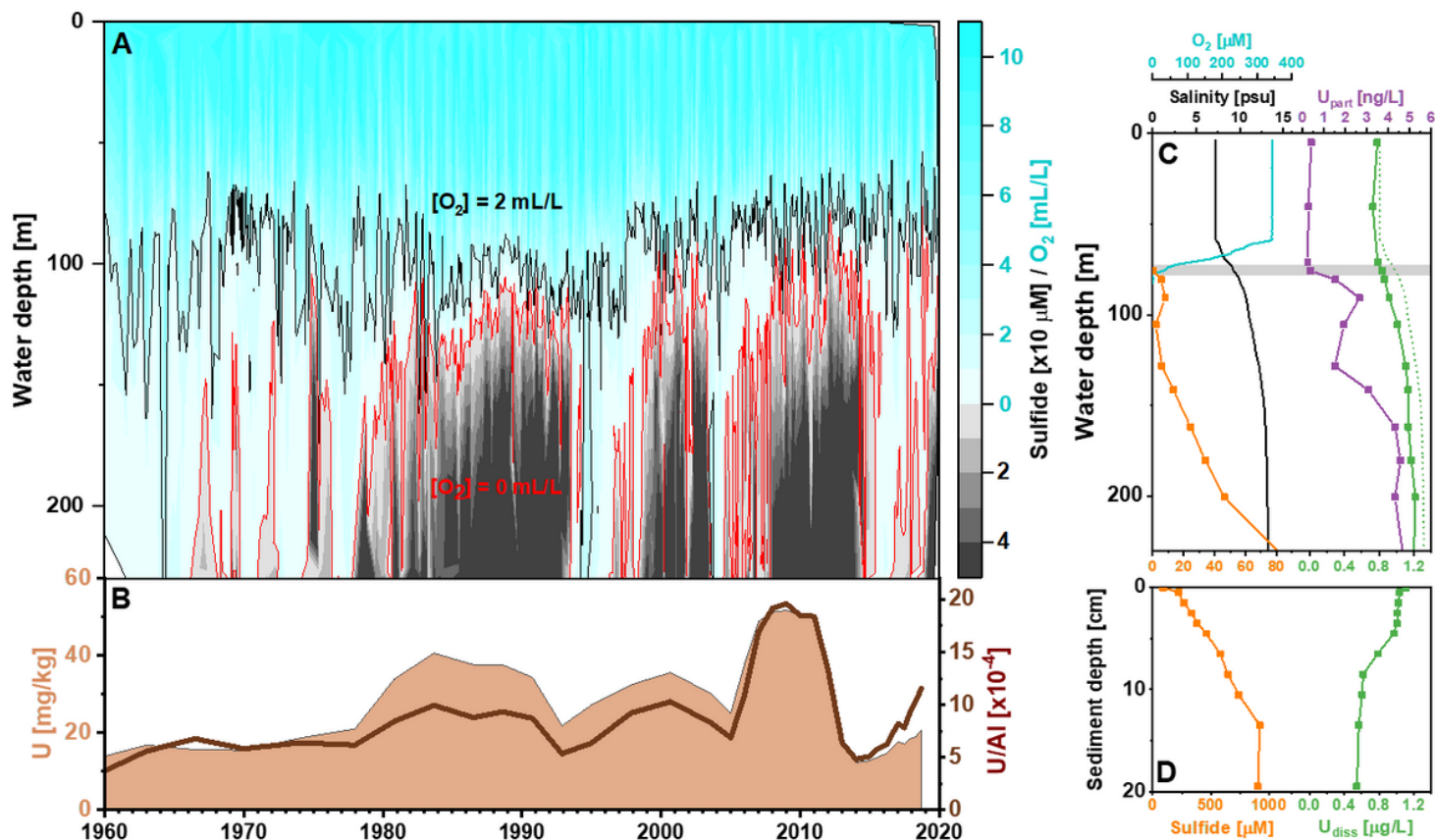


Figure 2

Comparison of water-column time series and the sedimentary record, as well as water column and pore water profiles from the Gotland Basin, Baltic Sea. (A) Instrumental water-column time series of O_2 and total sulfide in the Gotland Basin (ICES Dataset on Oceanography) 51; (B) Record of U contents in the sediment core 7-MUC4 collected at site GB7-4 (57°16.98'N, 20°07.23'E) in the Gotland Basin; (C) Profiles of salinity, concentrations of O_2 , total sulfide, particulate and dissolved U (green dot line = salinity-based U concentrations) in the water column at site GB271 (57°19.19'N, 20°02.52'E), which is very close to the site GB7-4; (D) Concentrations of total sulfide and dissolved U in the pore waters at site GB271. The grey bar in (C) represents the redoxcline ($O_2 < 3 \mu$ M and sulfide $< 0.2 \mu$ M) in the water column. The sediment core 7-MUC4, water column, and pore water samples were obtained during EMB201 cruise in December 2018.

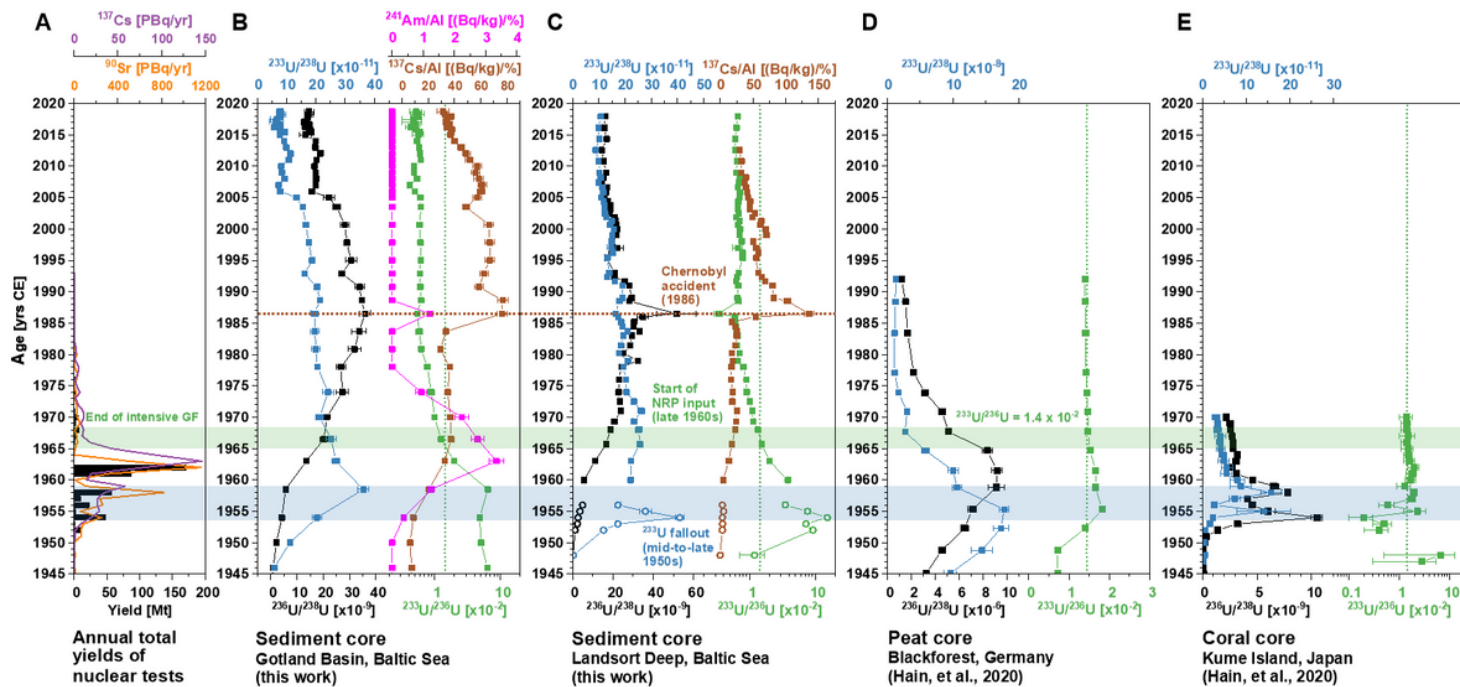


Figure 3

Comparison of ^{236}U and ^{233}U records. (A) Annual yields of nuclear tests and global depositions of ^{90}Sr and ^{137}Cs (UNSCEAR 2000) 50; (B) Records of $^{233}\text{U}/^{238}\text{U}$, $^{236}\text{U}/^{238}\text{U}$, $^{233}\text{U}/^{236}\text{U}$ atomic ratios, Al-normalized ^{137}Cs activities (decay-corrected to 2019) and ^{241}Am activities in the sediment core from the Gotland Basin (site GB7-4), Baltic Sea; (C) Records of $^{233}\text{U}/^{238}\text{U}$, $^{236}\text{U}/^{238}\text{U}$, $^{233}\text{U}/^{236}\text{U}$ atomic ratios, and Al-normalized ^{137}Cs activities (decay-corrected to 2019) in the composite sediment core from the Landsort Deep (site LD1), Baltic Sea; (D) Records of $^{233}\text{U}/^{238}\text{U}$, $^{236}\text{U}/^{238}\text{U}$, $^{233}\text{U}/^{236}\text{U}$ atomic ratios in a peat core from the Black Forest, Germany 14; and (E) Records of $^{233}\text{U}/^{238}\text{U}$, $^{236}\text{U}/^{238}\text{U}$, $^{233}\text{U}/^{236}\text{U}$ atomic ratios in a coral core from the Kume Island, Japan 14. The open circles and solid squares in (C) represent samples from core 36-MUC3 and 11-10MUC2, respectively. The $^{233}\text{U}/^{236}\text{U}$ atomic ratio in the peat core refers to the ratio of cumulative inventories of ^{233}U and ^{236}U below the referred layer.

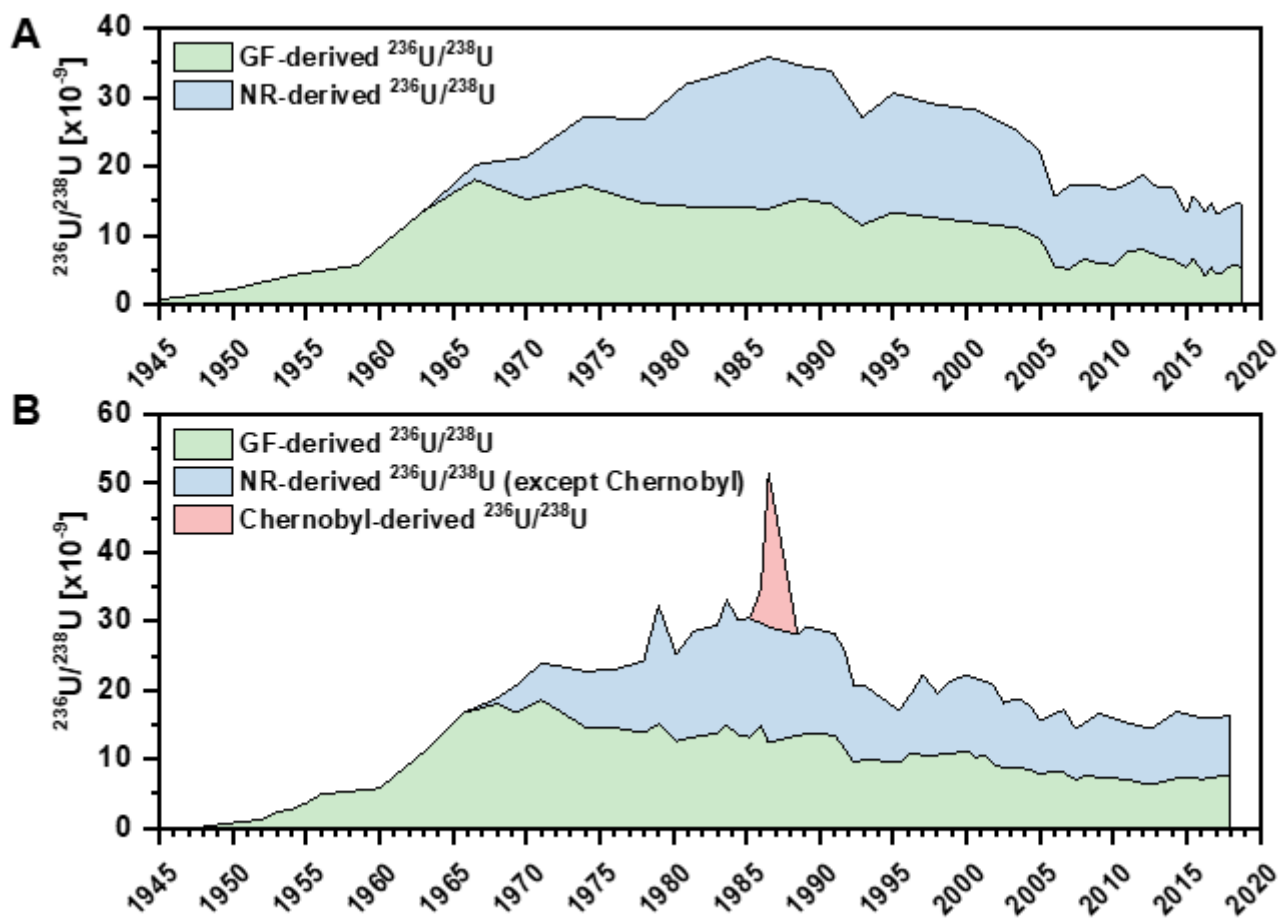


Figure 4

Sedimentary $^{236}\text{U}/^{238}\text{U}$ atomic ratios in the Gotland Basin (A) and Landsort Deep (B) allowing estimation on the contributions of different anthropogenic U sources. (GF: global fallout; NR: nuclear reactor)

Supplementary Files

This is a list of supplementary files associated with this preprint. Click to download.

- [SupportingInformationEST.docx](#)
- [TOCGraphic.png](#)